Lattice studies of pseudo-PDFs

Savvas Zafeiropoulos

Universität Heidelberg

13.03.2018

Galileo Galilei Institute for Theoretical Physics

In collaboration with J. Karpie (College of William & Mary), K. Orginos (College of William & Mary and JLAB), A. Radyushkin (ODU and JLAB)

From DIS to PDFs

- Since the discovery of quarks in DIS experiments at SLAC, PDFs always occupied a key role in HEP
- Large international effort aiming at their measurement
- Their measurement is actually possible due to factorization theorems

From DIS to PDFs

- Since the discovery of quarks in DIS experiments at SLAC, PDFs always occupied a key role in HEP
- Large international effort aiming at their measurement
- Their measurement is actually possible due to factorization theorems

From DIS to PDFs

- Since the discovery of quarks in DIS experiments at SLAC, PDFs always occupied a key role in HEP
- Large international effort aiming at their measurement
- Their measurement is actually possible due to factorization theorems

Factorization

Intuitively, factorization theorems (Collins, Soper and Sterman (1989)) tell us that the same universal non-perturbative objects (the PDFs), representing long distance physics, can be combined with many short-distance calculations in QCD to give the cross-sections of various processes.

- $\sigma = f \otimes H$, where f are the PDFs, H is the hard perturbative part and $\otimes$ is convolution.
- PDFs truly characterize the hadronic target
- essentially non-perturbative

Factorization

Intuitively, factorization theorems (Collins, Soper and Sterman (1989)) tell us that the same universal non-perturbative objects (the PDFs), representing long distance physics, can be combined with many short-distance calculations in QCD to give the cross-sections of various processes.

- $\sigma = f \otimes H$, where f are the PDFs, H is the hard perturbative part and $\otimes$ is convolution.
- PDFs truly characterize the hadronic target
- essentially non-perturbative

Factorization

Intuitively, factorization theorems (Collins, Soper and Sterman (1989)) tell us that the same universal non-perturbative objects (the PDFs), representing long distance physics, can be combined with many short-distance calculations in QCD to give the cross-sections of various processes.

- $\sigma = f \otimes H$, where f are the PDFs, H is the hard perturbative part and $\otimes$ is convolution.
- PDFs truly characterize the hadronic target
- essentially non-perturbative

Lattice ?

- The only ab-initio method to study QCD non-perturbatively is on the lattice. But ...
- PDFs are defined as an expectation value of a bilocal operator evaluated along a light-like line.
- Clearly, we can not evaluate this on a Euclidean set-up.

Lattice ?

- The only ab-initio method to study QCD non-perturbatively is on the lattice. But ...
- PDFs are defined as an expectation value of a bilocal operator evaluated along a light-like line.
- Clearly, we can not evaluate this on a Euclidean set-up.

Lattice ?

- The only ab-initio method to study QCD non-perturbatively is on the lattice. But ...
- PDFs are defined as an expectation value of a bilocal operator evaluated along a light-like line.
- Clearly, we can not evaluate this on a Euclidean set-up.

Lattice traditionally

- Calculation of Mellin moments of PDFs through matrix elements of twist-2 operators.
- Would not be an issue if every moment were accessible because a probability distribution is completely determined once all its moments are known.
- These studies are limited to the first few (three) moments due to
  - bad signal to noise ratio
  - power-divergent mixing on the lattice (discretized space-time does not possess the full rotational symmetry of the continuum).

Global PDF fits

- Realize a QCD analysis of hard-scattering measurements employing a variety of hadronic observables
- Parton densities parametrized @ an initial energy scale evolved up to the scale of data via DGLAP eqs.
- Build theoretical predictions for the observables.
- Best fit parameters determined by the minimization of an appropriate figure of merit (eg. χ^2).
- Many free parameters
- Advanced techniques (eg. use of neural networks).

Light-like is a NO-GO

- quasi-PDFs (X. Ji)
- pseudo-PDFs (A. Radyushkin)

Formalism

Computing PDFs in LQCD we start from the equal time hadronic matrix element with the quark and anti-quark fields separated by a finite distance.

For non-singlet parton densities the matrix element

$$\mathcal{M}^\alpha(z,p) \equiv \langle p|\bar{\psi}(0)\,\gamma^\alpha\,\hat{E}(0,z;A)\tau_3\psi(z)|p\rangle$$

where $\hat{E}(0,z;A)$ is the $0 \to z$ straight-line gauge link in the fundamental representation, τ_3 is the flavor Pauli matrix, and γ^a is a gamma matrix. We can decompose the matrix element due to Lorentz invariance as

$$\mathcal{M}^\alpha(z,p) = 2p^\alpha \mathcal{M}_p(-(zp),-z^2) + z^\alpha \mathcal{M}_z(-(zp),-z^2)$$

Formalism

From the $\mathcal{M}_p(-(zp), -z^2)$ part the twist-2 contribution to PDFs can be obtained in the limit $z^2 \to 0$. By taking $z = (0, 0, 0, z_3)$, α in the temporal direction i.e. $\alpha = 0$, and the hadron momentum $p = (p^0, 0, 0, p)$ the z^α-part drops out.

The Lorentz invariant quantity $\nu = -(zp)$, is the "Ioffe time" (Ioffe (1969), Braun (1994))

and

$$\langle p|\bar{\psi}(0)\,\gamma^0\,\hat{E}(0, z; A)\tau_3\psi(z)|p\rangle \;= 2p^0\mathcal{M}_p(\nu, z_3^2)$$

the quasi-PDF $Q(y, p)$ is related to $\mathcal{M}_p(\nu, z_3^2)$ by

$$Q(y, p) = \frac{1}{2\pi}\int_{-\infty}^{\infty} d\nu\; e^{-iy\nu}\,\mathcal{M}_p(\nu, [\nu/p]^2)$$

Formalism

Ioffe time PDFs $\mathcal{M}(\nu, z_3^2)$ defined at a scale $\mu^2 = 1/z_3^2$ are the Fourier transform of regular PDFs $f(x, \mu^2)$.

$$\mathcal{M}(\nu, z_3^2) = \int_{-1}^{1} dx\, f(x, 1/z_3^2) e^{ix\nu}$$

Scale dependence of the Ioffe time PDF derived from the DGLAP evolution of the regular PDFs.

Ioffe time PDFs evolution equation

$$\frac{d}{d \ln z_3^2} \mathcal{M}(\nu, z_3^2) = -\frac{\alpha_s}{2\pi} C_F \int_0^1 du\, B(u) \mathcal{M}(u\nu, z_3^2)$$

with $B(u) = \left[\frac{1+u^2}{1-u}\right]_+$ where $C_F = 4/3$, and $B(u)$ is the LO evolution kernel for the non-singlet quark PDF Braun (1994))

Obtaining the Ioffe time PDF

$z_3 << \rightarrow \mathcal{M}_p(\nu, z_3^2) = \mathcal{M}(\nu, z_3^2) + \mathcal{O}(z_3^2)$

But.... large $\mathcal{O}(z_3^2)$ corrections prohibit the extraction.

Conservation of the vector current implies $\mathcal{M}_p(0, z_3^2) = 1 + \mathcal{O}(z_3^2)$.

but in a ratio z_3^2 corrections (related to the transverse structure of the hadron) might cancel (Radyushkin (2017))

$$\mathfrak{M}(\nu, z_3^2) \equiv \frac{\mathcal{M}_p(\nu, z_3^2)}{\mathcal{M}_p(0, z_3^2)}$$

- much smaller $\mathcal{O}(z_3^2)$ corrections and therefore this ratio could be used to extract the Ioffe time PDFs
- a well defined continuum limit and does not require renormalization

Numerical implementation

First case study in an unphysical setup

- Quenched approximation
- $32^3 \times 64$ lattices with $a = 0.093$fm.
- $m_\pi = 601$MeV and $m_N = 1411$MeV

Now employing dynamical ensembles

a(fm)	M_π(MeV)	β	$L^3 \times T$
0.127(2)	440	6.1	$24^3 \times 64$
0.127(2)	440	6.1	$32^3 \times 96$
0.094(1)	280	6.3	$32^3 \times 64$

Table: Parameters for the lattices generated by the JLab/W&M collaboration using 2+1 flavors of clover Wilson fermions and a tree-level tadpole-improved Symanzik gauge action. The lattice spacings, a, are estimated using the Wilson flow scale w_0. Stout smearing implemented in the fermion action makes the tadpole corrected tree-level clover coefficient c_{SW} used, to be very close to the value determined non-pertubatively with the Schrödinger functional method

Numerical implementation

Following, Bouchard et al (2016)) we compute a regular nucleon two point function

$$C_p(t) = \langle \mathcal{N}_p(t)\overline{\mathcal{N}}_p(0)\rangle \,,$$

and $\quad C_p^{\mathcal{O}^0(z)}(t) = \sum_\tau \langle \mathcal{N}_p(t)\mathcal{O}^0(z,\tau)\overline{\mathcal{N}}_p(0)\rangle$ with $\mathcal{O}^0(z,t) = \overline{\psi}(0,t)\gamma^0\tau_3\hat{E}(0,z;A)\psi(z,t)$

Proton momentum and displacement of the quark fields along the $\hat{z}$ axis

$$\mathcal{M}_{\rm eff}(z_3 p, z_3^2; t) = \frac{C_p^{\mathcal{O}^0(z)}(t+1)}{C_p(t+1)} - \frac{C_p^{\mathcal{O}^0(z)}(t)}{C_p(t)}$$

Extract the desired m. e. $\mathcal{J}$ at large Euclidean time separation as $\frac{\mathcal{J}(z_3 p, z_3^2)}{2p^0} = \lim_{t\to\infty} \mathcal{M}_{\rm eff}(z_3 p, z_3^2; t)$, where p^0 is the energy of the nucleon.

Numerical implementation

- Renormalization of the m.e.?
- For $z_3 = 0$ $\mathcal{M}(z_3 p, z_3^2) \to$ the local iso-vector current, should be $= 1$ (but ...) lattice artifacts...
- Introduce an RC $Z_p = \frac{1}{\mathcal{J}(z_3 p, z_3^2)\big|_{z_3=0}}$
- Z_p has to be independent from p. But lattice artifacts or potential fitting systematics ...
- renormalize the m. e. for each momentum with its own $Z_p \to$ maximal statistical correlations to reduce statistical errors, and cancellation of lattice artifacts in the ratio

Numerical implementation

- Renormalization of the m.e.?
- For $z_3 = 0$ $\mathcal{M}(z_3 p, z_3^2) \to$ the local iso-vector current, should be $= 1$ (but ...) lattice artifacts...
- Introduce an RC $Z_p = \frac{1}{\mathcal{J}(z_3 p, z_3^2)\big|_{z_3=0}}$
- Z_p has to be independent from p. But lattice artifacts or potential fitting systematics ...
- renormalize the m. e. for each momentum with its own $Z_p \to$ maximal statistical correlations to reduce statistical errors, and cancellation of lattice artifacts in the ratio

Numerical implementation

- Renormalization of the m.e.?
- For $z_3 = 0$ $\mathcal{M}(z_3 p, z_3^2) \rightarrow$ the local iso-vector current, should be $= 1$ (but ...) lattice artifacts...
- Introduce an RC $Z_p = \frac{1}{\mathcal{J}(z_3 p, z_3^2)\big|_{z_3=0}}$
- Z_p has to be independent from p. But lattice artifacts or potential fitting systematics ...
- renormalize the m. e. for each momentum with its own $Z_p \rightarrow$ maximal statistical correlations to reduce statistical errors, and cancellation of lattice artifacts in the ratio

Numerical implementation

- Renormalization of the m.e.?
- For $z_3 = 0$ $\mathcal{M}(z_3 p, z_3^2) \to$ the local iso-vector current, should be $= 1$ (but ...) lattice artifacts...
- Introduce an RC $Z_p = \frac{1}{\mathcal{J}(z_3 p, z_3^2)\big|_{z_3=0}}$
- Z_p has to be independent from p. But lattice artifacts or potential fitting systematics ...
- renormalize the m. e. for each momentum with its own $Z_p \to$ maximal statistical correlations to reduce statistical errors, and cancellation of lattice artifacts in the ratio

Numerical implementation

- Renormalization of the m.e.?
- For $z_3 = 0$ $\mathcal{M}(z_3 p, z_3^2) \to$ the local iso-vector current, should be $= 1$ (but ...) lattice artifacts...
- Introduce an RC $Z_p = \frac{1}{\mathcal{J}(z_3 p, z_3^2)\big|_{z_3=0}}$
- Z_p has to be independent from p. But lattice artifacts or potential fitting systematics ...
- renormalize the m. e. for each momentum with its own $Z_p \to$ maximal statistical correlations to reduce statistical errors, and cancellation of lattice artifacts in the ratio

Numerical implementation

- in practise use the double ratio

$$\mathfrak{M}(\nu, z_3^2) = \lim_{t\to\infty} \frac{\mathcal{M}_{\text{eff}}(z_3 p, z_3^2; t)}{\mathcal{M}_{\text{eff}}(z_3 p, z_3^2; t)\big|_{z_3=0}} \times \frac{\mathcal{M}_{\text{eff}}(z_3 p, z_3^2; t)\big|_{p=0, z_3=0}}{\mathcal{M}_{\text{eff}}(z_3 p, z_3^2; t)\big|_{p=0}} ,$$

- infinite t limit is obtained with a fit to a constant for a suitable choice of a fitting range.

Numerical implementation

- in practise use the double ratio

$$\mathfrak{M}(\nu, z_3^2) = \lim_{t\to\infty} \frac{\mathcal{M}_{\text{eff}}(z_3 p, z_3^2; t)}{\mathcal{M}_{\text{eff}}(z_3 p, z_3^2; t)\big|_{z_3=0}} \times \frac{\mathcal{M}_{\text{eff}}(z_3 p, z_3^2; t)\big|_{p=0, z_3=0}}{\mathcal{M}_{\text{eff}}(z_3 p, z_3^2; t)\big|_{p=0}} ,$$

- infinite t limit is obtained with a fit to a constant for a suitable choice of a fitting range.

Results

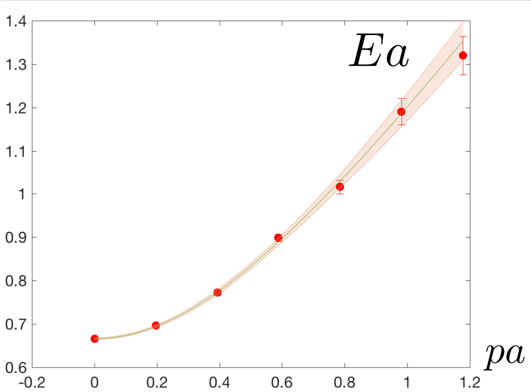

Nucleon dispersion relation. Energies and momenta are in lattice units. The solid line is the continuum dispersion relation (not a fit) while the errorband is an indication of the statistical error of the lattice nucleon energies

Results

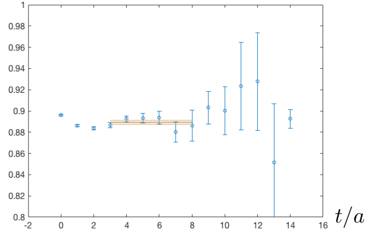

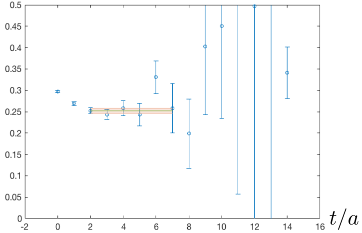

Typical fits used to extract the reduced matrix element (here $p = 2\pi/L \cdot 2$ and $z = 4$ (LHS) and $p = 2\pi/L \cdot 3$ and $z = 8$ (RHS)). The average χ^2 per degree of freedom was $\mathcal{O}(1)$. All fits are performed with the full covariance matrix and the error bars are determined with the jackknife method.

Results

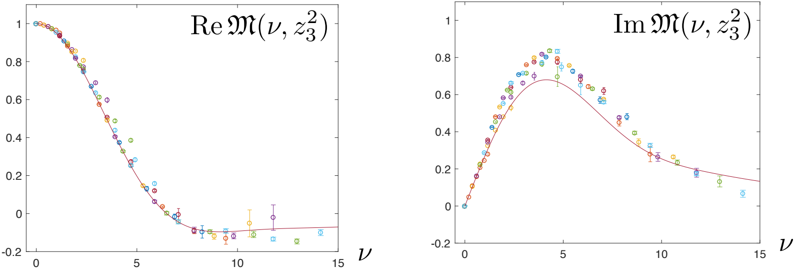

Re and Im parts of $\mathfrak{M}(\nu, z_3^2)$. Curves plotted for comparison, given by Re and Im Fourier trafos of $q_v(x) = \frac{315}{32}\sqrt{x}(1-x)^3$. The data are approximately described by the same curve. This phenomenon can be understood if an approximate factorization of the longitudinal and transverse structure of the hadron occurs.

Residual z_3-dependence

- Data plotted as a function of the Ioffe time we can see that there is a residual z_3-dependence.
- This is more visible when, for a particular $\nu \rightarrow$ several data points corresponding to different values of z_3.
- Different values of z_3^2 for the same ν correspond to the Ioffe time distribution at different scales.

Residual z_3-dependence

- Data plotted as a function of the Ioffe time we can see that there is a residual z_3-dependence.
- This is more visible when, for a particular $\nu \rightarrow$ several data points corresponding to different values of z_3.
- Different values of z_3^2 for the same ν correspond to the Ioffe time distribution at different scales.

Residual z_3-dependence

- Data plotted as a function of the Ioffe time we can see that there is a residual z_3-dependence.
- This is more visible when, for a particular $\nu \rightarrow$ several data points corresponding to different values of z_3.
- Different values of z_3^2 for the same ν correspond to the Ioffe time distribution at different scales.

Residual z_3-dependence

- Is the residual scatter in the data points consistent with evolution? By solving the evolution equation at LO, the Ioffe time PDF at z_3' is related to the one at z_3 by

$$\mathfrak{M}(\nu, {z'}_3^2) = \mathfrak{M}(\nu, z_3^2) - \frac{2}{3}\frac{\alpha_s}{\pi} \ln({z_3'}^2/z_3^2) \int_0^1 du\, B(u)\, \mathfrak{M}(u\nu, z_3^2)$$

- only applicable at small z_3
- Check its effect using data at values of $z_3 \leq 4a$ corresponding to energy scales larger than 500 MeV.
- We fix the point z_3' at the value $z_0 = 2a$ corresponding, at leading logarithm level, to the $\overline{\mathrm{MS}}$-scheme scale $\mu_0 = 1$ GeV and evolve the rest of the points to that scale.

Residual z_3-dependence

- Is the residual scatter in the data points consistent with evolution? By solving the evolution equation at LO, the Ioffe time PDF at z_3' is related to the one at z_3 by

$$\mathfrak{M}(\nu, {z'}_3^2) = \mathfrak{M}(\nu, z_3^2) - \frac{2}{3}\frac{\alpha_s}{\pi} \ln({z_3'}^2/z_3^2) \int_0^1 du\, B(u)\, \mathfrak{M}(u\nu, z_3^2)$$

- only applicable at small z_3
- Check its effect using data at values of $z_3 \leq 4a$ corresponding to energy scales larger than 500 MeV.
- We fix the point z_3' at the value $z_0 = 2a$ corresponding, at leading logarithm level, to the $\overline{\mathrm{MS}}$-scheme scale $\mu_0 = 1$ GeV and evolve the rest of the points to that scale.

Residual z_3-dependence

- Is the residual scatter in the data points consistent with evolution? By solving the evolution equation at LO, the Ioffe time PDF at z_3' is related to the one at z_3 by

$$\mathfrak{M}(\nu, {z'}_3^2) = \mathfrak{M}(\nu, z_3^2) - \frac{2}{3}\frac{\alpha_s}{\pi} \ln({z_3'}^2/z_3^2) \int_0^1 du\, B(u)\, \mathfrak{M}(u\nu, z_3^2)$$

- only applicable at small z_3
- Check its effect using data at values of $z_3 \leq 4a$ corresponding to energy scales larger than 500 MeV.
- We fix the point z_3' at the value $z_0 = 2a$ corresponding, at leading logarithm level, to the $\overline{\rm MS}$-scheme scale $\mu_0 = 1$ GeV and evolve the rest of the points to that scale.

Before and after evolution

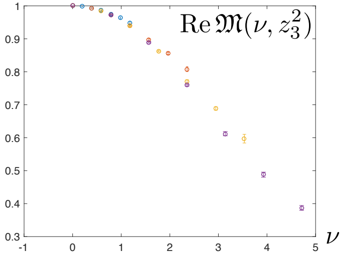

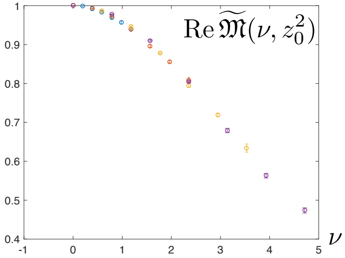

The ratio $\mathfrak{M}(\nu, z_3^2)$ for for $z_3/a = 1, 2, 3,$ and 4. **LHS:** Data before evolution. **RHS:** Data after evolution. The reduction in scatter indicates that evolution collapses all data to the same universal curve.

Before and after evolution

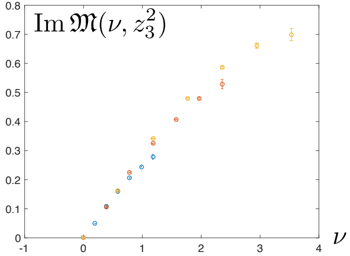

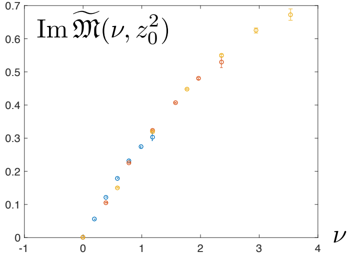

The ratio $\mathfrak{M}(\nu, z_3^2)$ for for $z_3/a = 1, 2, 3,$ and 4. **LHS:** Data before evolution. **RHS:** Data after evolution. The reduction in scatter indicates that evolution collapses all data to the same universal curve.

More on evolution

- LO evolution cannot be extended to very low scales.
- It is known that evolution stops below a certain scale (by observing our data we infer that this is the case for $z_3 \geq 6a$.)
- Adopt an evolution that leaves the PDF unchanged for length scales above $z_3 = 6a$ and use the leading perturbative evolution formula to evolve to smaller z_3 scales.

More on evolution

- LO evolution cannot be extended to very low scales.
- It is known that evolution stops below a certain scale (by observing our data we infer that this is the case for $z_3 \geq 6a$.)
- Adopt an evolution that leaves the PDF unchanged for length scales above $z_3 = 6a$ and use the leading perturbative evolution formula to evolve to smaller z_3 scales.

Comparison to global fits

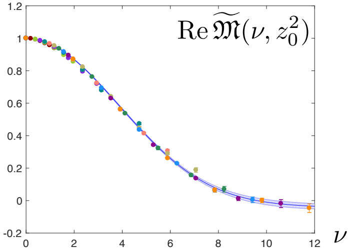

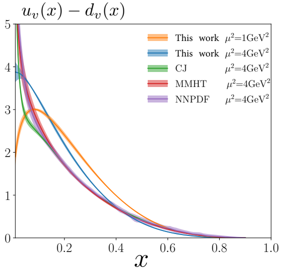

LHS: Data points for Re $\mathfrak{M}\,(\nu, z_3^2)$ with $z_3 \leq 10a$ evolved to $z_3 = 2a$. By fitting these evolved points with a cosine FT of $q_v(x) = N(a,b)x^a(1-x)^b$ we obtain $a = 0.36(6)$ and $b = 3.95(22)$ (statistical errors). RHS: Curve for $u_v(x) - d_v(x)$ built from the evolved data shown in the left panel and treated as corresponding to the $\mu^2 = 1$ GeV^2 scale; then evolved to the reference point $\mu^2 = 4$ GeV^2 of the global fits.

Conclusions and outlook

- We presented a new approach for obtaining PDFs from lattice QCD calculations
- Using an appropriate ratio of matrix elements we were able to get rid of UV divergences ensuring a well defined continuum limit
- one can scan in Ioffe time ν which is the Fourier dual to the momentum fraction x by using the hadron momentum
- large hadron momentum required to access the large ν-regime or equivalently small-x physics
- to approach the light cone we need to send $z_3^2 \to 0$ keeping ν fixed

Conclusions and outlook

- We presented a new approach for obtaining PDFs from lattice QCD calculations
- Using an appropriate ratio of matrix elements we were able to get rid of UV divergences ensuring a well defined continuum limit
- one can scan in Ioffe time ν which is the Fourier dual to the momentum fraction x by using the hadron momentum
- large hadron momentum required to access the large ν-regime or equivalently small-x physics
- to approach the light cone we need to send $z_3^2 \to 0$ keeping ν fixed

Conclusions and outlook

- We presented a new approach for obtaining PDFs from lattice QCD calculations
- Using an appropriate ratio of matrix elements we were able to get rid of UV divergences ensuring a well defined continuum limit
- one can scan in Ioffe time ν which is the Fourier dual to the momentum fraction x by using the hadron momentum
- large hadron momentum required to access the large ν-regime or equivalently small-x physics
- to approach the light cone we need to send $z_3^2 \to 0$ keeping ν fixed

Conclusions and outlook

- We presented a new approach for obtaining PDFs from lattice QCD calculations
- Using an appropriate ratio of matrix elements we were able to get rid of UV divergences ensuring a well defined continuum limit
- one can scan in Ioffe time ν which is the Fourier dual to the momentum fraction x by using the hadron momentum
- large hadron momentum required to access the large ν-regime or equivalently small-x physics
- to approach the light cone we need to send $z_3^2 \to 0$ keeping ν fixed

Conclusions and outlook

- The pseudo-PDF ratio lead to suppression of scaling violations in z_3^2
- The logarithmic singularity $(\ln(-z_3^2))$ of $\mathcal{M}(\nu, z_3^2)$ lead to DGLAP evolution
- The observed z^2 dependence is compatible with DGLAP evolution
- soon we will be finalizing our results with $2+1$ dynamical flavors of Wilson clover fermions which will include a more detailed study of all involved systematics (disretization effects, finite-volume effects, lighter pions etc)

Conclusions and outlook

- The pseudo-PDF ratio lead to suppression of scaling violations in z_3^2
- The logarithmic singularity $(\ln(-z_3^2))$ of $\mathcal{M}(\nu, z_3^2)$ lead to DGLAP evolution
- The observed z^2 dependence is compatible with DGLAP evolution
- soon we will be finalizing our results with $2+1$ dynamical flavors of Wilson clover fermions which will include a more detailed study of all involved systematics (disretization effects, finite-volume effects, lighter pions etc)

Conclusions and outlook

- The pseudo-PDF ratio lead to suppression of scaling violations in z_3^2
- The logarithmic singularity $(\ln(-z_3^2))$ of $\mathcal{M}(\nu, z_3^2)$ lead to DGLAP evolution
- The observed z^2 dependence is compatible with DGLAP evolution
- soon we will be finalizing our results with $2+1$ dynamical flavors of Wilson clover fermions which will include a more detailed study of all involved systematics (disretization effects, finite-volume effects, lighter pions etc)

Thanks a lot for your attention!!!